

Optical gating width variability using electrode parasitic capacitance

Atsushi Yamada^{1a)}, Yasuaki Nagashima², Shinichi Onuki²,
Yoshiharu Shimose², Akihito Otani², and Kenji Kawano²

¹ Anritsu Device Co., Ltd., 5–1–1 Onna, Atsugi-shi, Kanagawa 243–0032, Japan

² Anritsu Corporation, 5–1–1 Onna, Atsugi-shi, Kanagawa 243–8555, Japan

a) Atsushi.Yamada@anritsu.com

Abstract: We developed an optical gating device using a bulk layer and high mesa ridge/BH hybrid structure with input power of 14.5 dBm for optical communication performance monitoring. The shortest gating width of 3.9 ps was obtained in all-optical sampling experiments. However, gated waveform distortion occurred due to superfluous carriers in absorption layer in case of low bias voltage and optical pumping power condition. We have successfully improved waveform quality by extension electric parasitic capacitance to draw out it, thus variable gating width depending on transmission speed has been realized.

Keywords: optical switches, optical modulation

Classification: Integrated optoelectronics

References

- [1] E. Kehayas, *et al.*: “40-Gb/s All-Optical Processing Systems Using Hybrid Photonic Integration Technology,” *J. Lightwave Technol.* **24** (2006) 4903 (DOI: [10.1109/JLT.2006.884994](https://doi.org/10.1109/JLT.2006.884994)).
- [2] R. Akimoto, *et al.*: “Monolithically integrated all-optical gate switch using intersubband transition in InGaAs/AlAsSb coupled double quantum wells,” *Opt. Express* **19** (2011) 13386 (DOI: [10.1364/OE.19.013386](https://doi.org/10.1364/OE.19.013386)).
- [3] P. Li, *et al.*: “Low-Complexity TOAD-Based All-Optical Sampling Gate With Ultralow Switching Energy and High Linearity,” *IEEE Photon. J.* **7** [4] (2015) (DOI: [10.1109/JPHOT.2015.2459377](https://doi.org/10.1109/JPHOT.2015.2459377)).
- [4] I. Shake, *et al.*: “Simple Q factor monitoring for BER estimation using opened eye diagrams captured by high-speed asynchronous electrooptical sampling,” *IEEE Photonics Technol. Lett.* **15** (2003) 620 (DOI: [10.1109/LPT.2003.809316](https://doi.org/10.1109/LPT.2003.809316)).
- [5] T. Mori, *et al.*: “Double Pulse Pumping on All-Optical Sampling Using Electroabsorption Modulator,” *OFC (2010) OWF5* (DOI: [10.1364/OFC.2010.OWF5](https://doi.org/10.1364/OFC.2010.OWF5)).
- [6] T. Mori, *et al.*: “All-optical sampling using cross-absorption modulation in electroabsorption modulator for optical performance monitor,” *ECOC (2008) We.1.D.5* (DOI: [10.1109/ECOC.2008.4729283](https://doi.org/10.1109/ECOC.2008.4729283)).
- [7] K. Naoe, *et al.*: “43-Gbit/s operation of 1.55- μ m electro-absorption modulator integrated DFB laser modules for 2-km transmission,” *ECOC (2005) Th.2.6.4*.
- [8] N. Edagawa, *et al.*: “Novel Wavelength Converter Using an Electroabsorption Modulator,” *IEICE Trans. Electron.* **E81-C** (1998) 1251.

- [9] Y. Akage, *et al.*: “Wide bandwidth of over 50 GHz travelling-wave electrode electroabsorption modulator integrated DFB lasers,” *Electron. Lett.* **37** (2001) 299 (DOI: [10.1049/el:20010168](https://doi.org/10.1049/el:20010168)).
- [10] D. A. B. Miller, *et al.*: “Electric field dependence of optical absorption near the band gap of quantum-well structures,” *Phys. Rev. B* **32** (1985) 1043 (DOI: [10.1103/PhysRevB.32.1043](https://doi.org/10.1103/PhysRevB.32.1043)).
- [11] M. Suzuki, *et al.*: “InGaAsP electroabsorption modulator for high-bit-rate EDFA system,” *IEEE Photonics Technol. Lett.* **4** (1992) 586 (DOI: [10.1109/68.141976](https://doi.org/10.1109/68.141976)).
- [12] H. Soda, *et al.*: “High-speed GaInAsP/InP buried-heterostructure optical intensity modulator with semi-insulating InP burying layers,” *Electron. Lett.* **23** (1987) 1232 (DOI: [10.1049/el:19870858](https://doi.org/10.1049/el:19870858)).
- [13] A. Yamada, *et al.*: “High-mesa Ridge/BH Hybrid Structure Optical Gating Device based on Cross-Absorption Modulation of Electro-absorption Modulator,” *ECOC* (2011) We.10.P1.40 (DOI: [10.1364/ECOC.2011.We.10.P1.40](https://doi.org/10.1364/ECOC.2011.We.10.P1.40)).
- [14] T. Mori, *et al.*: “Variable Gate Width, All-Optical Sampling using Electro-absorption Modulator for Optical Performance Monitor,” *OFC* (2011) OWC3 (DOI: [10.1364/OFC.2011.OWC3](https://doi.org/10.1364/OFC.2011.OWC3)).

1 Introduction

An optical performance monitor (OPM) is required for transparent monitoring of optical networks. An optical sampling technique is effective to measure waveforms to assess the quality of high-speed modulation signals. An optical sampling gate [1, 2, 3] with short gating width and high extinction ratio is required for an OPM with high temporal resolution and signal-to-noise ratio. The electro-absorption modulator (EAM) based on cross absorption modulation (XAM) is a leading candidate for a compact optical sampling gate with high cost efficiency [4, 5, 6, 7, 8]. A standard EAM for light source has MQW structure absorption layer because of its the low operating voltage and highly efficient characteristics [9, 10], however it has drawbacks, such as high polarization dependency and narrow operating wavelength bandwidth for gating device. A bulk structure absorption layer is suitable to overcome these drawbacks [11, 12].

In this paper, we propose a hybrid structure with high-mesa waveguide and conventional p/n-InP BH for both facets regions. This structure, in which the BH region acts a thermal spreader, enables high power input, low transmission loss and polarization insensitivity [13]. The sampling system of variety transmission speed might be impacted by the gating width [14]. We found that the gated waveform exhibits a large tailing edge under low bias voltage and high pumping power. The superfluous carriers will be still remained in the absorption layer even by reverse bias, and they will prevent to change the transmission loss. Thus the buffer region is needed to store temporally the carriers in the layer. Further, we propose the structural design with a parasitic capacitance of electrode area to optimize the system speed.

2 Device structure

Fig. 1 shows a schematic of the high-mesa ridge/BH hybrid structure grown by MOVPE on n-InP substrate. Waveguide stripe was formed after fabricating absorption layer and cladding layer. Standard buried heterostructure layer was grown using a standard p/n-InP blocking layer, and then etched deeply to shape high-mesa ridge structure by wet chemical process. Wideband operation over the C-band, high extinction ratio of 35 dB and polarization insensitivity is required for gating device of OPM. 0.25 μm thickness, 1.45 μm composition bulk absorption layer as waveguide was used for absorption layer instead of MQW waveguide considering absorption peak shift under reverse bias voltage.

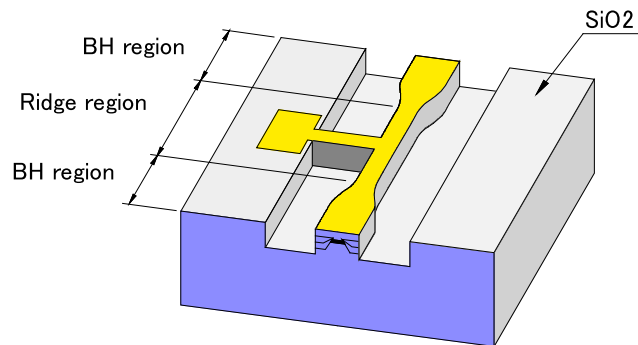


Fig. 1. Schematic of high mesa ridge/BH hybrid structure

The waveguide layer was designed to optimize total device loss including polarization dependent loss and scattering loss in the waveguide, coupling loss onto the single-mode fiber. The waveguide widths of ridge and BH region are 5.3 μm and 4 μm , device and BH region length are 250 μm and 60 μm , respectively. The taper region is placed at the boundary area in the BH region. Both front and rear facets are coated with single layer SiOx films. The fabricated module was mounted onto a small package with dimension of 25 (W) \times 36 (D) \times 9 (H) mm with two RF-input SMA connectors on each side of the case, and coupled to single mode fiber using single aspherical lens.

3 Static characteristics

The transmission loss was measured with a CW input of -10 dBm from a tunable light source over the input wavelength from 1510 nm to 1590 nm. Fig. 2 shows the voltage absorption characteristics from $+0.4$ to -8 V bias voltage and the polarization difference. A minimum transmission loss of 7.7 dB at $+0.4$ V bias and a maximum polarization dependency of 0.8 dB were obtained over the C-band. The transmission loss increased with applied voltage, and the extinction ratio exceeded 35 dB at -8 V bias.

Maximum input power of conventional EAM is limited up to around 0 dBm owing to thermal issue in absorption layer by excessive power. As BH region of the hybrid structure acts as a thermal spreader, maximum input power under the CW mode improve to 14.5 dBm. This value is large enough for usual optical gating device.

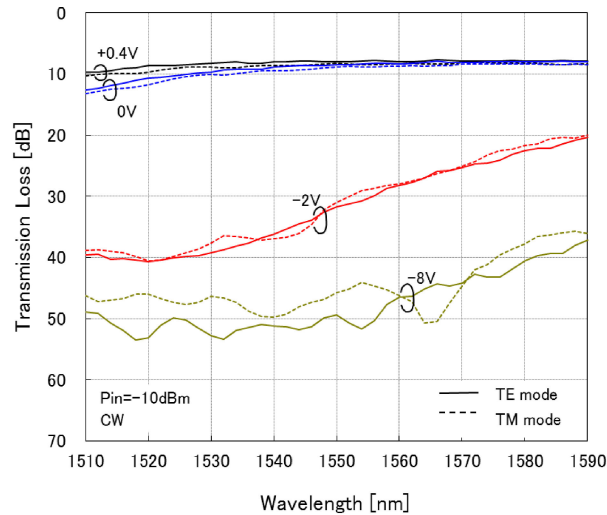


Fig. 2. Voltage absorption characteristics

4 All-optical sampling experiments

To investigate the optical gating performances of the fabricated module, we performed all optical sampling experiments. Since transmission loss is decreased by the injected pumping pulse based on XAM, the envelope of optical output pulse from the gating device is identical with waveform of the input short pulse. The pulse width and wavelength of the input optical short pulse in our experimental setup were 1.8 ps and 1546 nm, respectively. The pumping light wavelength was 1546 nm [13]. The gating width decrease with optical pumping pulse width and bias Voltage shown in Fig. 3, and the shortest gating width of 3.9 ps was achieved at a pumping pulse width of 3.4 ps and -10 V bias voltage as shown in Fig. 4. Although we also measured 5 Gbit/s modulation characteristic for external elec-

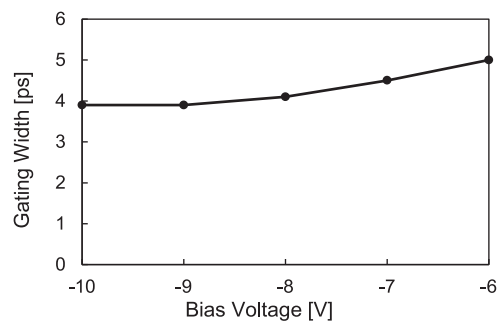


Fig. 3. Gating width characteristic

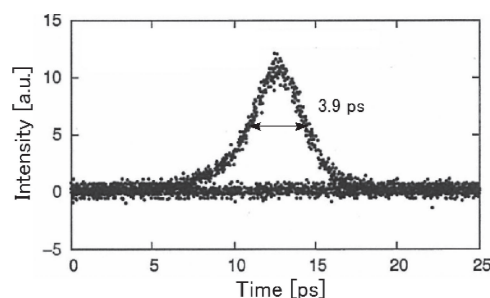


Fig. 4. Eye diagram with -10 V

trical signal in this device at -0.8 V bias, clear eye opening is not observed in optical eye diagram. On the other hand, clear gated waveform for optical pumping signal has been demonstrated. Low parasitic capacity is significant parameter for external modulation characteristic of EAM. In contrast, this is not important for gating device which is driven not by external electrical modulation, but by optical pumping. Hence high-speed response by external electrical modulation is not necessary for fast optical gating characteristic. A waveform tailing was seen in higher pumping pulse than 24 pJ and low bias voltage of -6 V , therefore we investigated the mechanism of the phenomenon.

5 Pumping power dependency

Fig. 5(a) shows experimental gating widths as a function of a pumping power at a bias voltage of -6 V . The maximum pumping power was then 46 pJ . The gating width enlarged and critical waveform tailing occur as increase of pumping power, and eventually gated waveform collapsed. Many superfluous carriers would occur with low reverse bias voltage and high pumping power condition. Reverse bias voltage could draws out generated carriers in absorption layer of the gating device. In case of too many generated carriers or low voltage condition, it assumes that the residual carriers will induce cause transmission loss tailing. In order to confirm this, we fabricated sample devices which increased electrode area from $80\text{ }\mu\text{m}$ square to $110 \times 130\text{ }\mu\text{m}$ (2.2 times) and $110 \times 210\text{ }\mu\text{m}$ (3.6 times). It was expected that parasitic capacitance of electrode extension performs as buffer region for superfluous carriers. All structure except electrode size is the same. Fig. 5(b), (c) shows gated waveform evaluation results with $110 \times 130\text{ }\mu\text{m}$ and $110 \times 210\text{ }\mu\text{m}$ electrode. Each row indicates same pumping power of 10 , 28 and 46 pJ from the top. In 2.2 times large electrode size, tailing phenomena is significantly improved, however small amount of tailing remained with 46 pJ pumping power. Finally, almost all

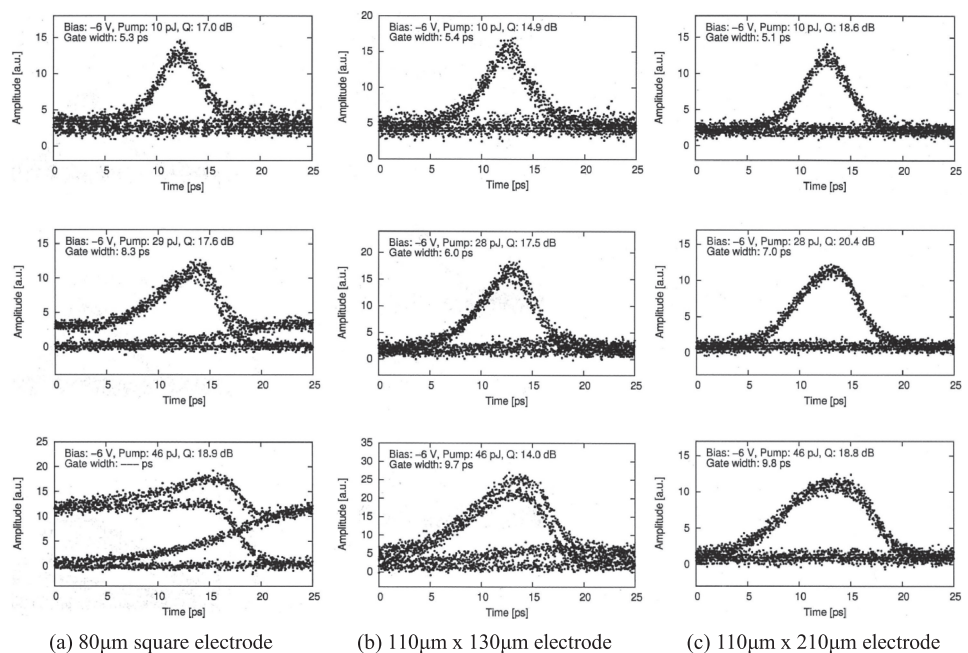


Fig. 5. Eye diagram with -6 V

tailing disappeared in 3.6 times large electrode. Gating width could change from 5.1 to 9.8 ps as pumping power without remarkable waveform collapse. It was confirmed that parasitic capacitance of electrode extension could performs as buffer for superfluous carriers.

6 Conclusion

We have successfully developed an optical gating device with high-mesa ridge/BH hybrid structure based on XAM of an EA modulator. Our device have high power input owing to heat spreader effect of BH structure and polarization insensitivity arising from a bulk absorption layer. The resulting input power of 14.5 dBm with low polarization dependency of 0.8 dB has been achieved. The gating width of 3.9 ps in the all-optical sampling system is established at a bias voltage of -10 V. The sampling system of variety transmission speed might be impacted by the gating width. The gated waveform showed undesired tailing edge arising from superfluous carriers in absorption layer under low bias voltage or high optical pumping power condition. Such undesired tailing edge could also be improved by employing a parasitic capacitance of expansion electrode area with $80\ \mu\text{m}$ square - $110\ \mu\text{m} \times 210\ \mu\text{m}$. We have successfully tuned the gating width within a time range from 5.1 ps–9.8 ps without any remarkable waveform transformation. The optical gating device using high mesa ridge/BH hybrid structure will provide us to develop the optical sampling systems with high times and cost efficiencies.

Acknowledgments

We would acknowledge productive suggestions from Prof. Omatsu and Prof. Tateda.